Solid State Communications 221 (2015) 9–13

Contents lists available at ScienceDirect

Solid State Communications

journal homepage: www.elsevier.com/locate/ssc

Magnetic, magnetocaloric properties and phenomenological model in amorphous $Fe_{60}Ru_{20}B_{20}$ alloy

A. Boutahar [a,*], H. Lassri [a], E.K. Hlil [b]

[a] LPMMAT, Université Hassan II-Casablanca, Faculté des Sciences Ain Chock, BP 5366 Mâarif, Casablanca, Morocco
[b] Institue Néel, CNRS et Université Joseph Fourier, BP 166, F-38042 Grenoble Cedex 9, France

ARTICLE INFO

Article history:
Received 20 May 2015
Received in revised form
28 June 2015
Accepted 12 August 2015
Communicated by E.V. Sampathkumaran
Available online 20 August 2015

Keywords:
A. Amorphous $Fe_{60}Ru_{20}B_{20}$ alloy
D. Magnetocaloric effect
D. Magnetic transition
D. Phenomenological model

ABSTRACT

Magnetic, magnetocaloric properties and phenomenological model of amorphous $Fe_{60}Ru_{20}B_{20}$ alloy are investigated in detail. The amorphous alloy has been synthesized using melt spinning method. The magnetic transition nature undergoes a second-order magnetic phase transition from ferromagnetic to paramagnetic states with a Curie temperature of 254 K. Basis on the thermodynamic Maxwell's relation, magnetic entropy change ($-\Delta S_M$) is calculated. Further, we also report a theoretical investigation of the magnetocaloric effect using a phenomenological model. The best model parameters and their variation with temperature and the magnetic field were determined. The theoretical predictions are found to agree closely with experimental measurements.

1. Introduction

Fe–B based amorphous alloys have been widely studied because they combine excellent combination both mechanical and magnetic properties [1–5]. Paulose et al. [6] showed that amorphous Fe_x-$Ru_{80-x}B_{20}$ alloys undergo interesting changes in magnetic behavior with Ru concentration and temperature. Furthermore, Lofland et al. [7] reported that $Fe_{80}Ru_{10}B_{10}$ is a concentrated spin glass while $Fe_{33}Ru_{33}B_{34}$ exhibits reentrant magnetism. To investigate the magnetocaloric effect MCE in such systems further the present work on $Fe_{60}Ru_{20}B_{20}$ alloy was under taken.

On the other hand, the giant magnetocaloric effect (MCE) was observed in materials with a first-order magnetic transition such as $LaFe_{13-x}Si_x$ [8], $Gd_5(Si,Ge)_4$ [9] and others [10]. However, it is difficult to use these materials for magnetic refrigeration mainly because they have very large thermal and magnetic-field hysteresis [11]. However, the positive characteristics of second order magnetic transition (SOMT) in amorphous materials are a low magnetic hysteresis, a high electrical resistivity, enhanced corrosion resistance, good mechanical properties, and a tunable T_C by varying the composition [12–13]. From this point of view, magnetic studies reveal that the $Fe_{60}Ru_{20}B_{20}$ alloy undergoes a SOMT.

In this paper, we have performed magnetic and magnetoclaoric properties around SOMT of amorphous $Fe_{60}Ru_{20}B_{20}$ alloy. To investigate the magnetic transition nature, the magnetization behavior around T_C was analyzed in terms of Landau theory and confirmed by Arrott plots curves. In addition, a phenomenological model is applied to predict the magnetocaloric properties.

2. Experimental

Amorphous $Fe_{60}Ru_{20}B_{20}$ alloy was prepared by the usual melt spinning technique using single roller quenching, in an atmosphere of argon. The resulting ribbons were typically 1 to 2 mm wide and 25 μm thick. X-ray diffraction was used to check the amorphous state of the alloy and no Bragg peaks were observed. The exact chemical composition was determined by electron probe microanalysis. The magnetization was measured by the extraction method with applied magnetic field up to 14 T. The Curie temperature (T_C) is defined as the inflection point of the derivative of the temperature dependence of magnetization curve in a field of 0.05 T.

3. Results and discussion

3.1. Magnetic properties

The temperature dependences of magnetization (M–T) for the $Fe_{60}Ru_{20}B_{20}$ alloy was measured under an applied field of 0.05 T in a temperature range of 5–320 K as shown in Fig. 1. To have a precise determination of the Curie temperature, the dM/dT versus T plot has been performed and reported in the inset of Fig. 1. The T_C is defined as the inflection point of the dM/dT curve and it is found to be around

* Corresponding author.
E-mail address: boutahar.fsac@gmail.com (A. Boutahar).

http://dx.doi.org/10.1016/j.ssc.2015.08.002
0038-1098/

254 K. We note that the $Fe_{80}B_{20}$ has a T_C of around 650 K, as reported by Lofland et al. [7]. Next, replacing Fe by Ru, causes a rearrangement of Fe–Fe distances promoting more antiferromagnetic (AFM) pairing which decreases significantly the Curie temperature. The competing interactions are also responsible for the disappearance of ferromagnetism (FM) in amorphous $Ru_xFe_{80-x}B_{20}$ alloy with Ru concentration as reported by Paulose et al. [6].

We also note that the M (T) curve displays a tail at low temperatures, which can be attributed to the presence of a minor AFM contribution in this system. Fig. 2 confirms that the magnetization of this alloy does not saturate in an applied field of 8 kOe and consequently, the magnetic structure is not collinear at low temperature in $Fe_{60}Ru_{20}B_{20}$ alloy and that a very large applied field is needed to achieve total alignment of spins.

To investigate the type of the magnetic phase transition, we use the Inoue–Shimizu s–d model [14,15], which has been widely used to discuss behaviors of several types of magnetocaloric materials.

According to Landau theory [14,15], the magnetic free energy F (M, H) versus magnetization and temperature can be expressed as:

$$F=\frac{1}{2}a(T)M^2+\frac{1}{4}b(T)M^4+\frac{1}{6}c(T)M^6-\mu_0MH. \quad (1)$$

The Landau coefficients are accessible through the equation of state linking M and the magnetic field:

$$a(T)M+b(T)M^3+c(T)M^5=\mu_0H. \quad (2)$$

The coefficients a (T), b (T) and c (T) depend on temperature with respect to the thermal variation of spin fluctuations amplitude and can be determined by fitting the isothermal magnetization data using the above equation. Examination of the free energy demonstrates that the parameter a (T) is always positive and would get a minimum value at the Curie temperature corresponding to a maximum of susceptibility. On the other hand, the order of magnetic transition is governed by the sign of b (T): the 1st order transition takes place if b $(T_C)<0$, while the 2nd order transition occurs when b $(T_C)\geq 0$. Besides, c (T) is positive at T_C and, in the other temperature regions, can be negative or positive. The values of Landau's coefficients are determined by fitting the magnetization curves to Eq. (2). Accordingly, b (T_C) was found to be positive for $Fe_{60}Ru_{20}B_{20}$ alloy studied here, indicating a 2nd character to the magnetic transition for the sample. Fig. 3 shows the temperature dependence of the Landau's parameters for the $Fe_{60}Ru_{20}B_{20}$ alloy. As explained above, a (T) was found positive with a minimum close to T_C and b (T_C) was found positive indicating the occurrence of a SOMT. As shown in Fig. 3, the value of Curie temperature T_C derived from thermomagnetic measurements is exactly that obtained from the $a(T)$ behavior. In order to confirm that present alloy showed second-order magnetic transitions, we have checked the Arrott plots (M^2 vs. H/M curves) at different temperatures in Fig. 4. For all isothermal curves, the slope of the Arrott plots is found to be positive confirming that the

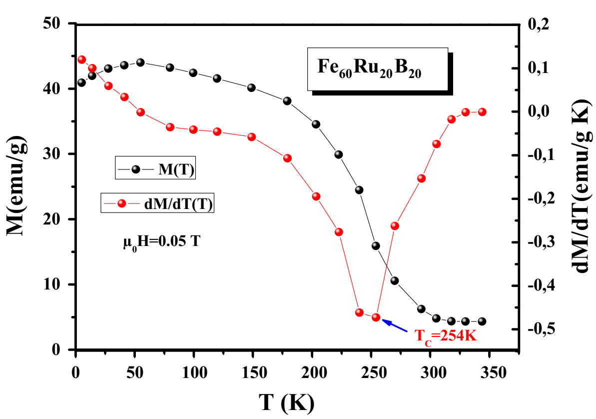

Fig. 1. Variation of magnetization and dM/dT as a function of temperature in an applied magnetic field of 0.05 T for the amorphous $Fe_{60}Ru_{20}B_{20}$ alloy.

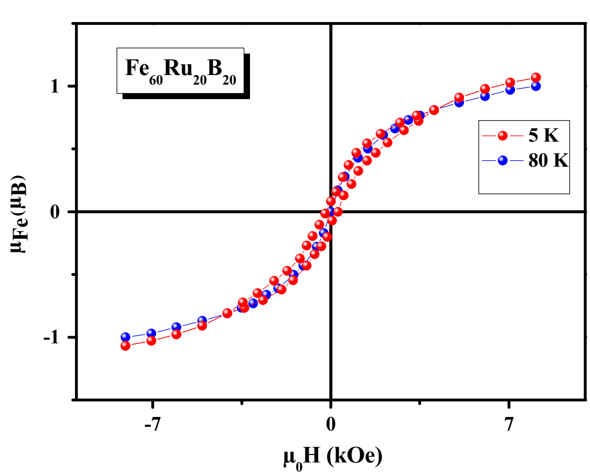

Fig. 2. Hysteresis loops of the amorphous $Fe_{60}Ru_{20}B_{20}$ alloy.

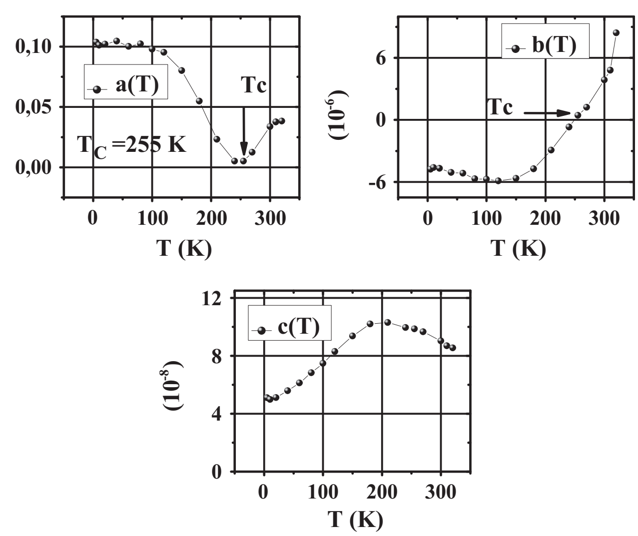

Fig. 3. Temperature dependence of Landau coefficients for the amorphous $Fe_{60}Ru_{20}B_{20}$ alloy. The units for $a(T)$, $b(T)$ and $c(T)$ are T^2 kg/J, T^4 kg^3/J^3, T^6 kg^5/J^5, respectively.

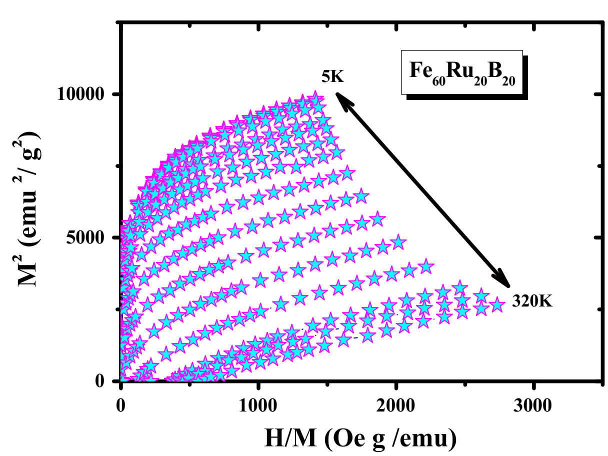

Fig. 4. Arrott plots of the amorphous $Fe_{60}Ru_{20}B_{20}$ alloy at different temperatures close to T_C.